

Simple Model of Electronic Density of States of Graphite and Its Application to the Investigation of Superlattices

Wing-Tat PONG and Colm DURKAN*

Nanoscience Centre, University of Cambridge, 11. J J Thomson Ave, Cambridge, CB3 0FF, UK

(Received January 13, 2005; accepted March 2, 2005; published July 26, 2005)

A model of graphite which is easy to comprehend and simple to implement for the simulation of scanning tunneling microscopy (STM) images is described. This model simulates the atomic density of graphite layers, which in turn correlates with the local density of states. The mechanism and construction of such a model is explained with all the necessary details which have not been explicitly reported before. This model is applied to the investigation of rippling fringes which have been experimentally observed on a superlattice, and it is found that the rippling fringes are not related to the superlattice itself. A superlattice with abnormal topmost layers interaction is simulated, and the result affirms the validity of the moiré rotation pattern assumption. The “odd-even” transition along the atomic rows of a superlattice is simulated, and the simulation result shows that when there is more than one rotated layer at the top, the “odd-even” transition will not be manifest.

[DOI: 10.1143/JJAP.44.5365]

KEYWORDS: graphite, superlattice, moiré rotation pattern, rippling fringes, odd even transition

1. Introduction

Scanning probe microscopy investigations have extensively used graphite as a substrate due to its chemical inertness and ease of cleaving. The atomically flat surface of graphite has provided an ideal platform for surface scientists to deposit various kinds of materials of interest for imaging and examining. The natural graphite surface is worthy of further understanding as it contains a variety of defects,¹⁾ among which superlattice structures have been observed a number of times, whose origin is not yet completely understood.²⁾

A superlattice is a hexagonal lattice structure with triangular symmetry, with its periodicity usually several to tens of nanometers and its corrugation around several angstroms to a nanometer. Kuwabara *et al.* has proposed the moiré rotation pattern assumption to explain the origin of superlattices, and eq. (1) relates the periodicity P of a superlattice to its rotation angle θ between two graphite layers

$$P = \frac{d}{2 \sin(\theta/2)}, \quad (1)$$

where d is the atomic lattice constant.³⁾ Kobayashi has suggested another mechanism that nanoscale features a few layers underneath the surface can propagate through many layers without decay to explain superlattice formation.⁴⁾ Although there is still no clear conclusion on the origin of superlattices, the moiré rotation pattern should have a role in the formation of superlattices since Rong *et al.*⁵⁾ and Xhie *et al.*²⁾ have shown that the moiré pattern equation [eq. (1)] can properly describe the experimental results of the periodicity of the superlattice and the rotation angle by directly imaging the related atomic lattice vectors with the STM. Therefore, it is of paramount importance to investigate the origin of superlattices from the moiré rotation pattern assumption point of view.

In order to achieve this, a simulation model of a moiré rotation-induced superlattice would be indispensable since a superlattice cannot be experimentally prepared beforehand,

as it happens randomly. Without a simulation model, it would be difficult to amass data for analysis. Having been applied first in molecular dynamic simulations,⁶⁾ this model has been used to study superlattices a number of times.^{7–9)}

2. Simulation Model

The model is based on a formula which describes a continuous hexagonal lattice similar to the atomic lattice of graphite.^{6,7)} This formula has appeared in refs. 6–8, however, explanation and description on its formation was not reported before. Here we describe all the necessary details of the mechanism and construction of this model and the way we simulate the relative shift between the alternating layers. The atomic density of a layer n , Φ_n , at a position (x, y) is:

$$\begin{aligned} \Phi_n = 1 - \frac{2}{9} & \left[\cos \left[\left(\frac{2\pi}{2.46} \right) \left(x'' + \frac{y''}{\sqrt{3}} \right) \right] \right. \\ & + \cos \left[\left(\frac{2\pi}{2.46} \right) \left(x'' - \frac{y''}{\sqrt{3}} \right) \right] \\ & \left. + \cos \left[\left(\frac{4\pi}{2.46} \right) \left(\frac{y''}{\sqrt{3}} \right) \right] + \frac{3}{2} \right] \end{aligned} \quad (2)$$

In eq. (2), there are three key cosine components with their directions described by the vectors A , B , and C in Fig. 1,

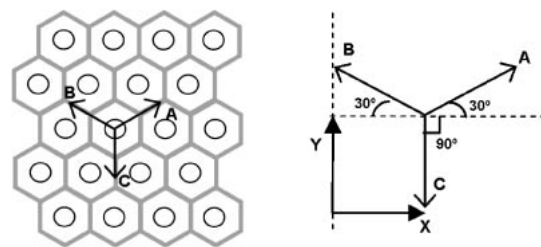


Fig. 1. Vectors A , B , C represent the directions of the three key cosine components in eq. (2). They point to three different directions which are 120° separated from each other, and their functions describe the hexagonal lattice. Vectors X , Y are the unit vectors, with which the vectors A , B , C can be formed as in eqs. (3)–(5). The atomic density variation along directions A , B , C is approximately sinusoidal, which can be simulated by the cosine functions in eq. (2).

*Corresponding author. E-mail address: cd229@eng.cam.ac.uk

and they correspond to the three vectors describing the hexagonal lattice and pointing to three different directions which are 120° separated from each other. Vectors \vec{X} and \vec{Y} (see Fig. 1) are unit vectors directed to the X and Y directions, and they are the component vectors for vectors \vec{A} , \vec{B} , and \vec{C} [eqs. (3)–(5)].

$$\vec{A} = \vec{X} + \tan 30^\circ \cdot \vec{Y} = \vec{X} + \frac{\vec{Y}}{\sqrt{3}} \quad (3)$$

$$\vec{B} = -\vec{X} + \tan 30^\circ \cdot \vec{Y} = -\vec{X} + \frac{\vec{Y}}{\sqrt{3}} \quad (4)$$

$$\vec{C} = -\sqrt{1^2 + \left(\frac{1}{\sqrt{3}}\right)^2} \cdot \vec{Y} = \frac{2}{\sqrt{3}} \vec{Y} \quad (5)$$

Starting from the beginning of the vectors and propagating along the vector directions, the varying atomic density can be approximately simulated by a cosine function with a period of 2.46 \AA . The offset of $3/2$ at the end inside the bracket is to shift the whole function above zero value while the $2/9$ at the front of the square bracket is for normalizing the bracket function. The operation of “1-” at the very front is to make such a function in phase with the actual atomic density variation. To build up a layered structure of graphite, more than one layer needs to be modeled. However, bear in mind that there is a relative shift between the alternating layers (see Fig. 2). This can be taken care of by modifying x, y in eqs. (6) and (7) so that the centre is shifted from C1 to C2. In regard to the rotation of graphite layers which will happen in a superlattice, eqs. (8) and (9) integrate the rotation angle into the model by rotating the coordinates with an angle θ .

$$x' = x + \Delta x = x + 1.42 \times \cos 30^\circ \quad (6)$$

$$y' = y + \Delta y = y + 1.42 \times \sin 30^\circ \quad (7)$$

$$x'' = x' \cos \theta - y' \sin \theta \quad (8)$$

$$y'' = x' \sin \theta + y' \cos \theta \quad (9)$$

3. Applications to Superlattices

A superlattice structure on graphite can be simulated with this model for various kinds of investigations. First of all, we

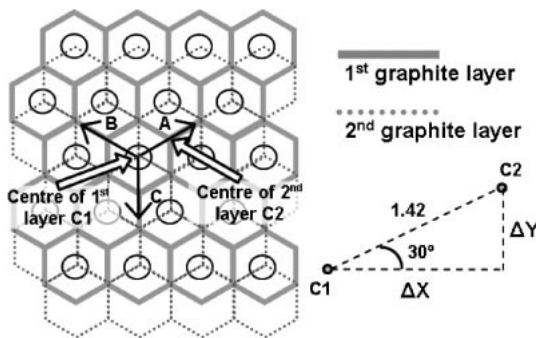


Fig. 2. The relative shift between alternating graphite layers is as shown. The centre of the 2nd layer C2 is displaced from the centre of the 1st layer C1 by a distance of 1.42 \AA with the displacement of Δx along X direction and Δy along Y direction. The angle 30° is found by simple geometry from the hexagonal lattice structure. With the x and y coordinates modified by Δx and Δy as in eqs. (6)–(7), the shift can be integrated into the model.

show that by using this model, the atomic lattice and superlattice structures of graphite can be simulated as observed under the STM. Then, we apply it to the investigations of the rippling fringes of the superlattice which we observed on graphite. One of the unusual aspects of superperiodic features on graphite proposed by Cee *et al.*⁷⁾ is compared with our corresponding simulation results. The “odd-even” transition along the atomic rows of the graphite atomic lattice on which a superlattice is superimposed, is simulated and investigated to observe how this transition phenomenon evolves as the periodicity of the superlattice changes.¹¹⁾

3.1 Modeling of superlattice structure

A superlattice can be modeled as two graphite layers with a rotation angle between them. Simulations of STM images generally entail including the effect of a third layer underneath the first two. There is a different weighting for each layer depending on the contribution of each layer to the overall structure. In normal cases, 1, 0.5, and 0.125 (normal weightings) are used for the 1st, 2nd, and 3rd layers respectively to reflect the assumption that the influence of a layer should decay with its depth from the surface.⁸⁾ By adding the atomic density contribution of each layer together, an STM image can be simulated with the intensity, I , at a point (x, y) as:

$$I(x, y) = \Phi_1(x, y) - W_2 \Phi_2(x, y) + W_3 \Phi_3(x, y), \quad (10)$$

where Φ_n is the atomic density of layer n , and W_2 and W_3 are the weightings representing the relative contribution of the 2nd and 3rd layers. Figures 3(a) and 3(b) are the $20 \text{ nm} \times 20 \text{ nm}$ superlattice area simulated with a rotation angle of 1st layer of 2.5° , $W_2 = 0.5$ and $W_3 = 0.125$. The three-fold symmetry of a superlattice is shown as observed under the STM.

3.2 Rippling fringes on superlattice

We have observed rippling fringes on a HOPG superlattice in our STM experiments. Those rippling fringes in the central part of Fig. 4(a) on the superlattice are of periodicity around 30 nm and corrugation 0.15 nm . In order to study whether the rippling fringes are related to the superlattice, a $400 \text{ nm} \times 400 \text{ nm}$ superlattice area, which resembles the one in Fig. 4(a) where the rippling fringes appear, is simulated with the normal weightings and with a rotation angle of 2.56° [Fig. 4(b)]. The simulated area is flat with the superlattice structure but without any large-scale features which can be associated with those rippling fringes in Fig. 4(a). We have performed the simulations with translational dislocations, and still we cannot observe any kind of fringes existing in the simulation result. Therefore the rippling fringes on the graphite are not due to an electronic effect of the superlattice and they are not part of the superlattice itself. One possible explanation for those rippling fringes is the physical buckling of the surface due to the intralayer strain. We believe this arises because the graphene sheet is bounded on three sides (laterally) by graphene sheets at different orientations, and also this sheet is rotated with respect to the substrate. This large degree of mismatch causes strain which can be relieved in the layer by buckling.

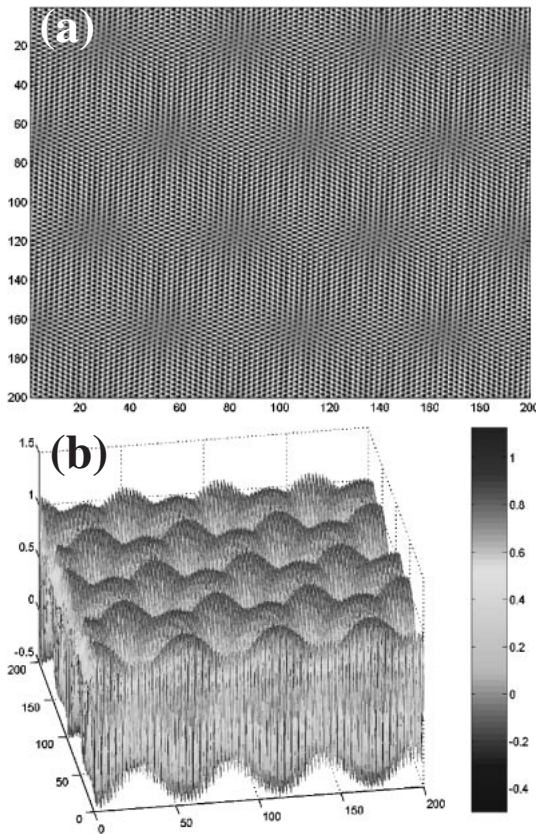


Fig. 3. (a) The 2-dimensional image of the 20 nm × 20 nm superlattice with a rotation angle of 2.5° (periodicity 5.64 nm) is simulated with $W_2 = 0.5$ and $W_3 = 0.125$. The bright area is higher than the dark area. (b) 3D image of the 20 nm × 20 nm superlattice in Fig. 3(a). The three-fold symmetry is obvious in Fig. 3(b) where the height difference between alternating peaks is discernible.

3.3 Investigation on the unusual aspect of superlattice proposed by Cee *et al.*⁷⁾

Cee *et al.* have simulated a superlattice, and reported that by using the exaggerated weightings of $W_2 = 0.125$ and $W_3 = 0.25$ which are counterintuitive in the respect of the moiré rotation pattern, a better contrast and three-fold symmetry can be obtained on the simulated superlattice. We have performed the same simulation with these weightings and the same rotation angle of 5° but we obtain different results. The difference in contrast in the simulated superlattice between using the normal weightings ($W_2 = 0.5$ and $W_3 = 0.125$) [Fig. 5(c)] and the exaggerated weightings ($W_2 = 0.125$ and $W_3 = 0.25$) [Fig. 5(d)] is not very significant. Cee *et al.* did not specify in their paper how they simulated the relative shift between alternating graphite layers which may be the reason for the difference between their results and ours. That is why we make the details of the simulation model explicit in §2 which were not clearly explained in the literature before, so that other workers can compare their results with ours. Also the difference in contrast would be more appropriately shown when the simulation results are displayed in 3D with the same absolute vertical scale. We found that the atomic lattice of the superlattice generated with the exaggerated weightings [Fig. 5(b)] does not have as obvious three-fold symmetry as that generated with the normal weightings [Fig. 5(a)], and

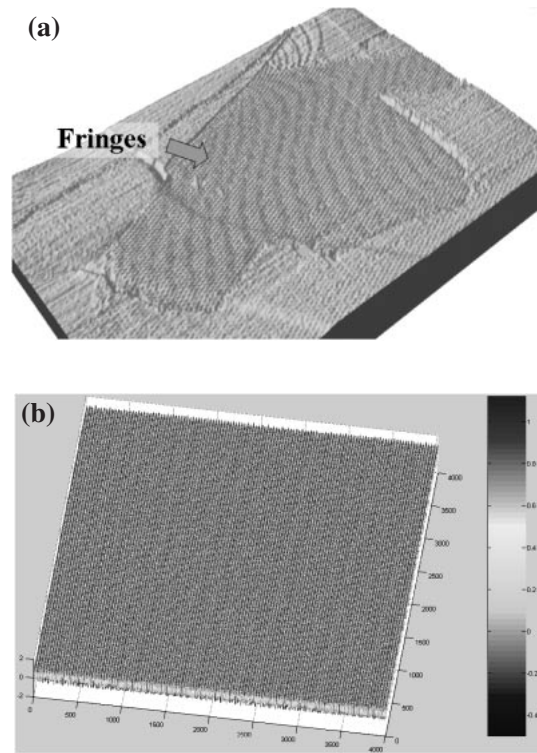


Fig. 4. Simulation of the rippling fringes on the superlattice of graphite. (a) The STM image of 700 nm × 500 nm ($I_t = 0.36$ nA, $V_s = 450$ mV) on graphite wherein we can observe the rippling fringes with periodicity of around 30 nm and corrugation 0.15 nm on the superlattice with a rotation angle of around 2.56° (periodicity 5.51 nm). (b) A superlattice with similar size and rotation angle is simulated with the normal weightings. However, there are no comparable rippling fringes in the simulation result.

indeed, it is difficult to observe the three-fold symmetry in Fig. 5(b). This is expected because the three-fold symmetry of the atomic lattice arises from the α and β sites on a graphite surface which in turn are due to the subtraction of the electronic density of states of the second graphite layer from the first; by using the exaggerated weightings of $W_2 = 0.125$ (instead of 0.5 for normal weightings), the effect of the subtraction is significantly diminished. Therefore, our simulation results show that the normal weightings which are consistent with the moiré rotation pattern assumption can generate a more physically realistic graphite atomic lattice and superlattice structures. The validity of the moiré rotation pattern assumption is asserted by our simulation model in this case.

3.4 “Odd-even” transition along atomic rows

It has been observed that when a superlattice structure is superimposed onto the underlying atomic lattice, the “odd-even” transition, which is a shift along an atomic row, will be manifested on the graphite surface (Fig. 12 in ref. 10). Osing *et al.* have proposed that such a transition will only occur if there is only one single layer rotated, thus it can be used as a criterion for determining whether the number of rotated layers is more than one.¹¹⁾ Osing’s proposal has been proved by our simulation results [Fig. 6(a)] which show that when there are two rotated layers, the “odd-even” transition will not be manifested, whereas the transition phenomenon will be obvious if there is only one rotated layer [Fig. 6(b)].

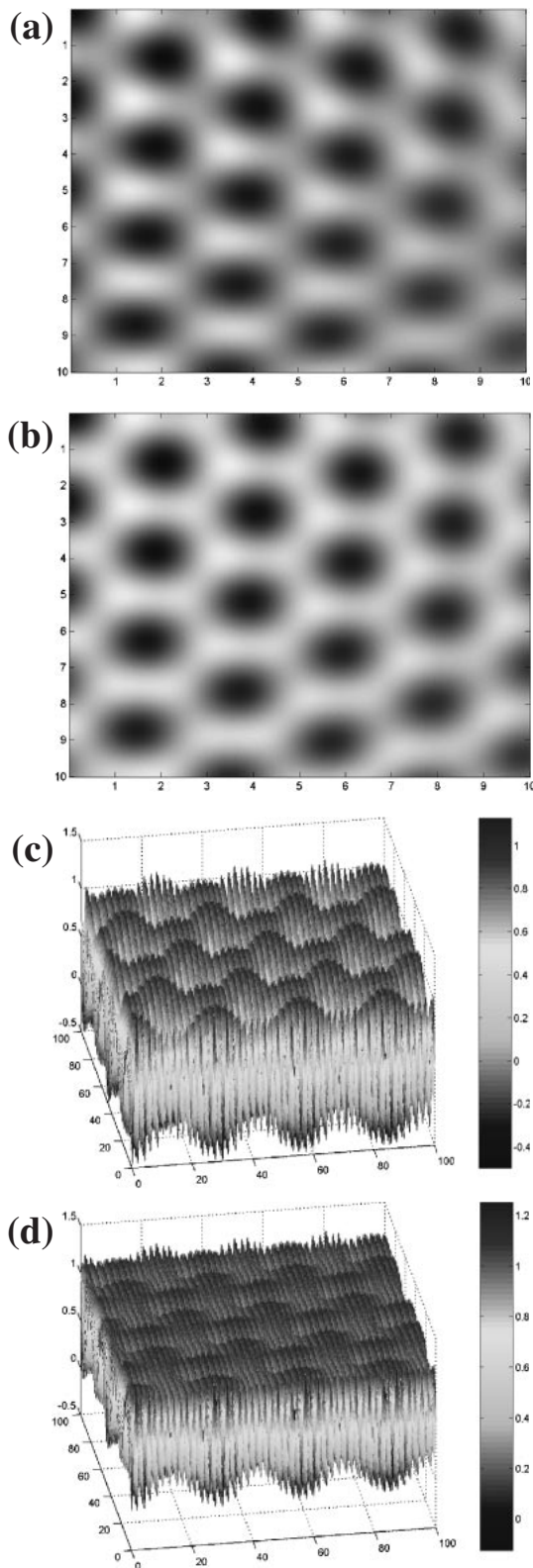


Fig. 5. Comparisons between the normal weightings and exaggerated weightings. (a) 1 nm^2 superlattice area simulated with the normal weightings. (b) 1 nm^2 superlattice area simulated with the exaggerated weightings. (c) 10 nm^2 superlattice area simulated with the normal weightings. (d) 10 nm^2 superlattice area simulated with the exaggerated weightings. All rotation angles are 5° (periodicity 2.82 nm). The three-fold symmetry of the atomic lattice is more distinct in Fig. 5(a) than in Fig. 5(b). The contrast in height is higher in Fig. 5(c) than in Fig. 5(d).

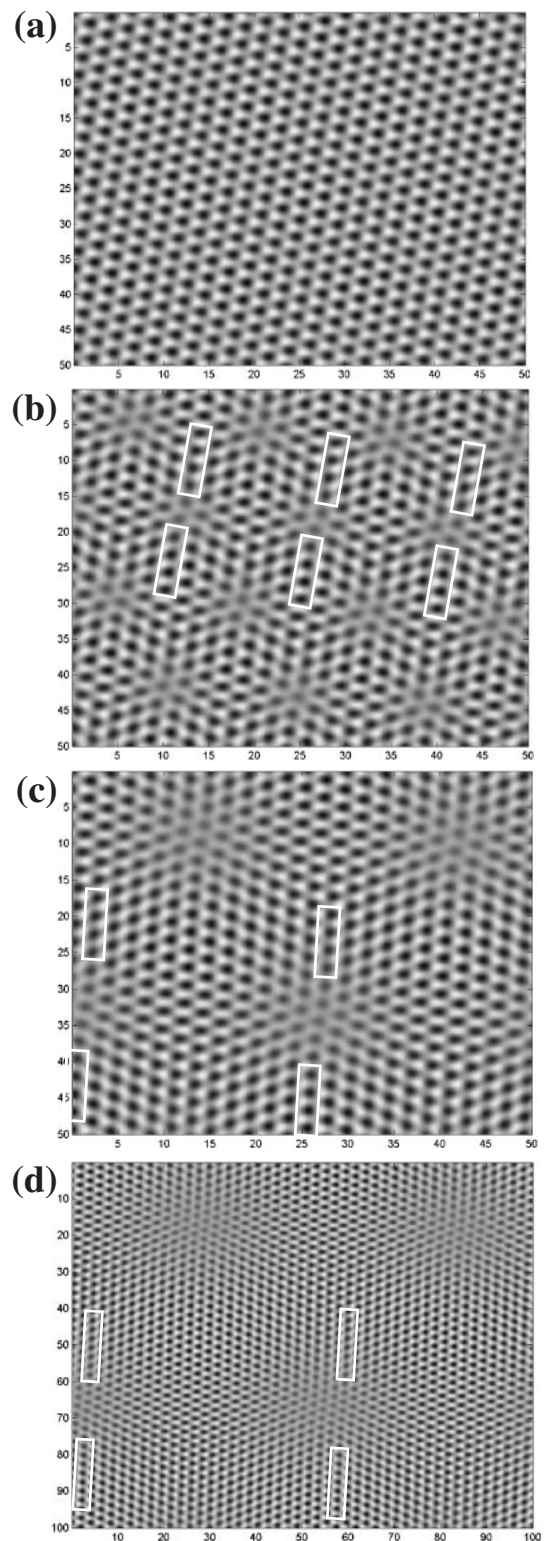


Fig. 6. “Odd-even” transition phenomenon on superlattice. (a) 5 nm^2 superlattice area with 1st and 2nd layers rotated by 10° relative to 3rd layer and periodicity of 1.41 nm . (b) 5 nm^2 superlattice area with 1st layer rotated by 10° relative to 2nd and 3rd layers and periodicity of 1.41 nm . (c) 5 nm^2 superlattice area with 1st layer rotated by 5° relative to 2nd and 3rd layers and periodicity of 2.82 nm . (d) 10 nm^2 superlattice area with 1st layer rotated by 2.5° relative to 2nd and 3rd layer and periodicity of 5.64 nm . All images are simulated with the normal weightings of $W_2 = 0.5$ and $W_3 = 0.125$. Osing’s proposal of the “odd-even” transition is proven by the simulation results shown in Fig. 6(a) and Fig. 6(b) where only Fig. 6(b) shows the transition. As the periodicity increases from Fig. 6(b) to Fig. 6(d), the transition phenomenon gets smeared out over distance.

We have investigated the influence of the periodicity of a superlattice on its “odd-even” transition phenomenon. From our simulation results, it is found that as the periodicity of the superlattice increases, the transition will be less significant due to the fact that the transition occurs over a longer distance and thus gets smeared out [see Figs. 6(b)–6(d)]. In the STM scanning, as the scanning size increases, the effect of thermal drift is likely to have a role in the images, and therefore, it would be difficult to decide, if the transition exists, whether it is due to the single layer rotation or thermal drift, especially, when the scan size is more than, for example, 10 nm.

4. Conclusion

Here we describe a model for graphite layers and its applications in investigating superlattice structures as have been observed by numerous STM experiments. This model is shown to be a powerful tool for analyzing various kinds of superlattice phenomena, which is important for the research of superlattice whose origin is yet not totally understood. Our simulations show different results from those of ref. 7, however they are consistent with the moiré rotation pattern assumption. The “odd-even” transition phenomenon and the theory by Osing *et al.* are shown and proven in this work.

Our simulation works on superlattices with zigzag shaped boundary,¹²⁾ a screw dislocation,⁹⁾ and a gradual change of periodicity will be reported later.

Acknowledgment

The authors thank for the research funding from the European Union IST project “QIPDDF-ROSES”.

- 1) C. R. Clemmer and T. P. Beebe Jr.: *Science* **251** (1991) 640.
- 2) J. Xhie, K. Sattler, M. Ge and N. Venkateswaran: *Phys. Rev. B* **47** (1993) 15835.
- 3) M. Kuwabara, D. R. Clarke and D. A. Smith: *Appl. Phys. Lett.* **56** (1990) 2396.
- 4) K. Kobayashi: *Phys. Rev. B* **53** (1996) 11091.
- 5) Z. Y. Rong and P. Kuiper: *Phys. Rev. B* **48** (1993) 17427.
- 6) R. Hentschke, B. Schurmann and J. Rabe: *J. Chem. Phys.* **96** (1992) 6213.
- 7) V. J. Cee, D. L. Patrick and T. P. Beebe Jr.: *Surf. Sci.* **329** (1995) 141.
- 8) H. Sun, Q. Shen, J. Jia, Q. Zhang and Q. Xue: *Surf. Sci.* **542** (2003) 94.
- 9) B. Feddes, I. I. Kravchenko and L. E. Seiberling: *Scanning* **20** (1998) 376.
- 10) B. Nysten, J. C. Roux, S. Flandrois, C. Daulan and H. Saadaoui: *Phys. Rev. B* **48** (1993) 12527.
- 11) J. Osing and I. V. Shvets: *Surf. Sci.* **417** (1998) 145.
- 12) K. Miyake, K. Akutsu, T. Yamada, K. Hata, R. Morita, M. Yamashita and H. Shigekawa: *Ultramicroscopy* **73** (1998) 185.